J. Water Environ. Nanotechnol., 8(1): 66-78 Winter 2023

ORIGINAL RESEARCH PAPER

Catalytic and Electrochemical Sensing Studies of Silver/Poly(1-Naphthylamine) Nanocomposites Synthesised by a Green Method

Femina Kanjirathamthadathil Saidu[1, 2], Alex Joseph[3], Eldhose Vadakkechalil Varghese[3], George Vazhathara Thomas [1,*]

[1] *Department of Chemistry, St. Joseph's College, Moolamattom, Idukki, Kerala 685591, India*
[2] *Department of Chemistry, Maharaja's College, Ernakulam, Kerala, 682011, India*
[3] *Department of Chemistry, Newman College, Thodupuzha, Kerala, 685584, India*

Received: 2022-09-17 Accepted: 2022-12-09 Published: 2023-02-12

ABSTRACT

Metal nanoparticles incorporated in conducting polymer nanocomposites have outstanding properties and potential applications in various fields and significant research has been carried out over the last two decades for the development of efficient methods for their synthesis. The current study describes a microwave-assisted, rapid, and environmentally friendly method for depositing silver nanoparticles (AgNPs) over poly(1-naphthylamine) (PNA) using clammy cherry (Cordia Obliqua willd) extract as a reductant to create silver/nanocomposites (Gr-Ag/PNA) with varying silver contents. Thermal stability and charge transfer kinetics of PNA was significantly improved upon introducing AgNPs, as evidenced by the thermogravimetric analysis and electrochemical investigations, respectively. All prepared Gr-Ag/PNA nanocomposites could show improved catalytic activity towards the borohydride-aided reduction of 4-nitrophenol (4-NP) and the pseudo-first-order rate constants showed a direct relationship with the percent of silver incorporated over PNA. Additionally, for the first time, the Gr-Ag/PNA modified carbon paste electrode (Gr-Ag/PNA/CPE) was utilized to validate its usefulness and applicability in the electrocatalytic reduction of 4-NP. A low-cost enzymeless voltammetric 4-NP sensor based on Gr-Ag/PNA/CPE was fabricated and it showed excellent selectivity for 4-NP, as well as a strong linear response over a wide range of 4-NP concentrations (30-1000 μM) and a detection limit of 6.25 μM.

Keywords: Green synthesis, Silver nanoparticles, Conducting polymers, Sensing, Catalyst

How to cite this article
Saidu F. K., Joseph A., Varghese E. V., Thomas G. V., Catalytic and Electrochemical Sensing Studies of Silver/Poly(1-Naphthylamine) Nanocomposites Synthesised by a Green Method. J. Water Environ. Nanotechnol., 2023; 8(1): 66-78
DOI: 10.22090/jwent.2023.08.007

INTRODUCTION

Metal nanoparticles (MNPs) are interesting nanofillers for futuristic applications because of their distinctive optoelectronic, electrical, and electrochemical properties. Spreading silver nanoparticles (AgNPs) across a support matrix can prevent metal leaching and particle aggregation, and enhance their catalytic and sensing potential. Carbon nanotubes, graphene oxide, graphene, metal sulfides, metal oxides, and similar materials have l been employed as solid supports for stabilizing and dispersing MNPs.[1–7]

Interestingly, conjugated polymers could work well as a support matrix for many MNPs, and their unique interactions between the components could lead to high activity, selectivity, and reproducibility, especially in catalytic and electrochemical sensing applications. Conjugated polymers, such as polypyrrole, polyaniline, polythiophene, and many others, have recently been used as the MNPs' support for the preparation of excellent sensors and catalysts.[8–12]

Remarkably, polyaniline and its derivatives have gained extensive research importance because of their ultra-porous structure, large specific surface area, chemical stability, and tunable

* Corresponding Author Email: *georgevtsjc@gmail.com*

electrochemical properties [13–17]. Poly(1-naphthylamine) abbreviated as PNA is a polyaniline derivative and possesses better thermal stability, excellent electrochemical properties, easy solution processability, and better adsorption and film-forming properties compared to polyaniline [18–22]. Recently, various PNA-based nanocomposites having enhanced photocatalytic, adsorption, and electrocatalytic performances were prepared upon incorporating selective nanofillers over PNA support [23–30][31].

The contamination of water resources by aromatic compounds like phenols and nitro-compounds like 4- nitrophenol (4-NP) synthetic dyes etc are increasing day by day causing a serious threat to the ecosystem since they are non-biodegradable and mutagenic and these carcinogenic compounds [32, 33]. For the effective management of 4-NP pollution, selective and sensitive monitoring of 4-NP is essential. The electrochemical methods using MNP-modified electrodes were established as reliable, reproducible, and cost-effective for 4- NP detection [17, 34, 35]. Additionally, such metal–conjugated polymer composites are active catalysts and have been widely explored as heterogeneous catalysts for the effective removal of pollutants like nitrophenols and synthetic dyes via reductive degradation [36–39].

The MNPs are usually incorporated over solid support by the reduction of metal ions in the presence of a dispersed support matrix, by chemical reductants such as borohydrides or hydrazine. Recently, the fast reduction of metal ions to MNPs in presence of various phytochemicals as eco-friendly reducing and capping agents has been explored as a green and economical alternative for the preparation of MNPs and their composites [40–42]. Our previous work reported that the phytochemicals present in the aqueous extract of clammy cherry were efficient in reducing and producing highly stable AgNPs at a faster rate under microwave (MW) activation [43].

Herein, AgNPs dispersed PNA nanocomposites were prepared by an MW-assisted reduction of silver ions in the presence of nano/microspheres of PNA using clammy cherry fruit extract as the non-toxic reducing agent. Different analytical tools were employed to establish the structural and physicochemical properties of prepared nanocomposites. Green synthesized Ag/PNA nanocomposites (Gr-Ag/PNA) were used as the electrode modifiers and electrocatalytic reduction and electrochemical sensing studies of 4-NP were performed. Moreover, the catalytic efficacy of prepared Gr-Ag/PNA towards the reductive discoloration of 4-NP with excess sodium borohydride was also investigated. The present study has explored a novel green route for the synthesis of PNA nanocomposites and its potential applications in pollution monitoring and remediation.

EXPERIMENTAL

Materials and methods.

The chemicals like silver nitrate ($AgNO_3$), nitric acid (HNO_3), ammonium peroxodisulphate (APS), potassium chloride (KCl), sodium hydroxide (NaOH), sodium hydrogen phosphate ($NaH_2PO_4.2H_2O$), sodium dihydrogen phosphate ($NaHPO_4.2H_2O$), sulphuric acid (H_2SO_4), sodium borohydride ($NaBH_4$), graphite powder, and 4-nitrophenol (4-NP), paraffin liquid, used in the study were of analytical grade and bought from Merck, India. 1-Naphthylamine (NA) was purchased from Loba Chemie, India and it was purified by recrystallization from ethanol. Distilled ethanol and deionized water are used as solvents for the present study. AgNPs and nanocomposite synthesis were carried out in a microwave oven (wave (LG) model 1S2021CW at 2450 MHz).

Preparation of Gr-Ag/PNA nanocomposites

PNA was synthesized by oxidative polymerization of NA by APS using the previously described method [29]. Ripened clammy cherries were taken from the campus of Maharaja's College, Ernakulam, Kerala, India, and clammy cherry extract (0.1 gL^{-1}) was made following the method reported earlier [43]. Three different PNA nanocomposites containing varying silver content say 5%, 10%, and 20 % were made by MW-assisted method using clammy cherry as the green reductant, and the resulting composites were designated as Gr-Ag-5/PNA, Gr-Ag-10/PNA and Gr-Ag-20/PNA respectively were 'Gr' refers for green synthesized. In a typical preparation for Gr-Ag-5/PNA, 1 g of dry PNA powder was probe-sonicated in 100 mL of deionized water. To this PNA dispersion, 5 mL of 0.1 M $AgNO_3$ solution was added in drops and magnetically stirred for 30 minutes. 20 mL of clammy cherry extract was then slowly added to this mixture. After 30 minutes of stirring, the mixture was placed in an MW oven at

350 W for 10 minutes. The resultant dispersion was further magnetically swirled for 30 minutes, cooled, filtered, washed, and dried, and the blackish-blue colored Gr-Ag-5/PNA powder was obtained. The aforesaid technique was performed with 10 mL and 20 mL of 0.1 M $AgNO_3$ solution, to prepare Gr-Ag-10/PNA, and Gr-Ag-20/PNA, respectively.

Characterization

The FTIR spectra of PNA and Gr-Ag/PNA nanocomposites were recorded in the range of 400–4,000 cm^{-1} with a NICOLET FT-IR Thermo scientific spectrometer, and XRD was performed with a Bruker AXS D8 advance diffractometer using CuK radiation (wavelength 1.5418 nm between 30°- 80°). HRTEM images of AgNPs, PNA, and Gr-Ag/PNA were recorded with the JOEL JEM2100 instrument. The OXFORD XMX N was used for energy dispersive X-ray analysis (EDAX), and the Perkin Elmer STA 6000-USA was used for thermogravimetric investigations of PNA and Gr-Ag/PNA nanocomposites at a temperature range of 50°C to 700°C under N_2 environment at a scan rate of 10°C/min. Thermo scientific evolution 1600 UV-vis spectrometer was used to record electronic spectra in the 200-800 nm range.

Electrochemical studies

The electrochemical analysis was performed in a three-electrode electrochemical setup with AUTOLAB galvanostat/potentiostat-model No.302N, Germany where Ag/AgCl was used as the reference electrode, Pt as the counter electrode and bare carbon paste electrode (CPE) or PNA or Gr-Ag/PNA modified CPE as working electrode. The CPE was prepared and modified with PNA and Gr-Ag/PNA nanocomposites by adopting the method reported by our research group earlier [29]. The PNA and three Gr-Ag/PNA modified CPE were represented as PNA/CPE and Gr-Ag-5/PNA/CPE, Ag-10/PNA/CPE, and Ag-20/PNA/CPE, respectively. The electrochemical response and charge transfer characteristics of the bare CPE, PNA/CPE, and the three Gr-Ag/PNA/CPEs were assessed by electrochemical impedance spectroscopy (EIS) and cyclic voltammetry (CV) studies.

The electrocatalytic reduction of 4-NP over bare CPE, PNA/CPE, and (Gr-Ag/PNA-20)/CPE was evaluated by CV in phosphate buffer (pH 7.0). The linear range and detection limit for Gr-Ag/PNA-20)/CPE-based 4-NP sensor was determined by differential pulse voltammetry (DPV) conducted in a potential range of 0 V to -0.7 V vs Ag/AgCl electrode at a pulse amplitude of 50 mV.

Catalytic reduction of 4-NP

The reduction of 4-NP with excess $NaBH_4$ was used as a model test to investigate the catalytic action of the produced Gr-Ag/PNA nanocomposites. In a typical process, a round-bottomed flask was taken with 20 mL of 4-NP solution (10^{-4} M). 5 mg of Gr-Ag-5/PNA nanocomposite was added to the above solution, sonicated, and then 5 mL of 0.05 M $NaBH_4$ was added and stirred. At regular intervals, suitable quantities of the reaction mixture were taken. The catalyst was separated by high-speed centrifugation, and the UV – visible spectrum was recorded. The entire study was repeated with other nanocomposites and pristine PNA to compare their catalytic activities.

RESULTS AND DISCUSSIONS

MW- assisted green synthesis of Gr-Ag/PNA nanocomposites

The present study used an aqueous extract of clammy cherry and MW irradiation to develop a faster and environmentally sustainable approach for the introduction of AgNPs onto the PNA surface. It has been reported that clammy cherry extract contains various polyfunctional compounds, and the reducing and stabilizing efficacy of clammy cherry-derived phytochemicals has already been validated in our past findings [43, 44]. MW irradiation accelerated the reduction of metal ions to AgNPs, and AgNPs with SPR band at around λ_{max} = 415 nm were obtained which confirmed the formation of AgNPs with an average size of 5-20 nm (Supplemental Fig. S1).

FTIR spectral studies

Fig. 1 shows the FTIR spectra of PNA and Gr-Ag/PNA nanocomposites. Stretching vibrations of hydrogen-bonded N–H bonds are associated with a wide band detected about 3335 cm^{-1} in all spectra. The sharp peak at 764 cm^{-1} detected in all spectra is attributed to C-H out-of-plane bending vibrations, and it validates polymerization through the 1,4 coupling of NA units, according to previous research [27]. In the FTIR spectra of all composites, peaks corresponding to imine stretching (1656 cm^{-1}) and quinonoid skeletal vibration (1586 cm^{-1}) were visible; however, the relative intensities of these peaks are shown to vary during nanocomposite

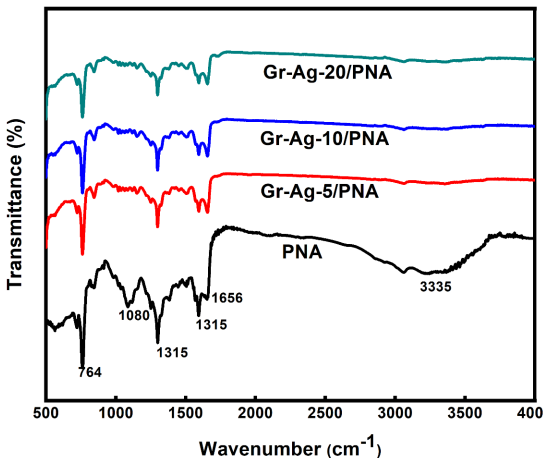

Fig. 1. FTIR spectra of PNA and Gr-Ag/PNA nanocomposites

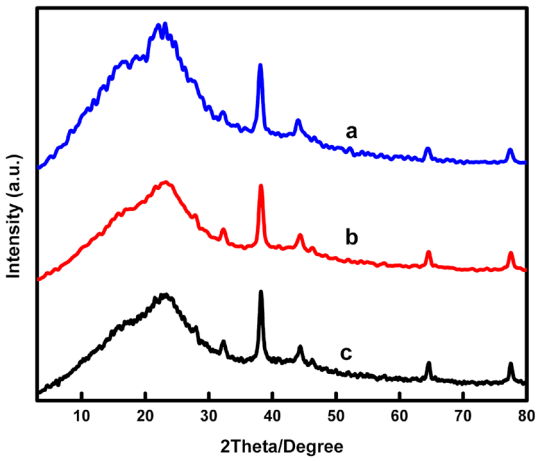

Fig. 2. XRD pattern of (a) Gr-Ag-5/PNA, (b) Gr-Ag-10/PNA and (c) Gr-Ag-20/PNA

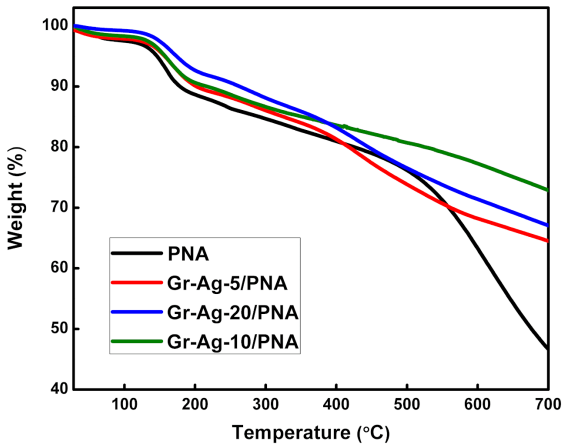

Fig. 3. TGA profile of PNA (a), Gr-Ag-5/PNA(b) Gr-Ag-10/PNA(c) and Gr-Ag-20/PNA(d) nanocomposites

production. PNA has a peak at 1315 cm^{-1} that is connected to C-N stretching vibrations of benzenoid-quinonoid units in the polymer backbone, and Gr-Ag/PNA nanocomposites have a significant change in the C-N stretching peak position. The presence of exclusive interactions between AgNPs and PNA was confirmed by the observed change in intensity and peak position.

XRD studies

The presence of a wide reflection from the (020) plane of PNA at about 23° in the XRD patterns of Gr-Ag/PNA nanocomposites (Fig. 2) suggested that PNA was mostly amorphous in the composite [29]. Additional intense diffractions were found for Gr-Ag/PNA nanocomposites that are characteristic of metallic silver, confirming the incorporation of silver over PNA, and there is an apparent rise in the intensities of the silver peak relative to that of PNA as the silver loading was increased. The peaks at 37.7°, 44.3°, 64.7°, and 77.6° are assigned to the [1 1 1], [2 0 0], [2 2 0], and [3 1 1] crystal planes of the metallic silver of fcc structure, respectively (JCPDS No;04-0783).

Thermogravimetric analysis (TGA)

TGA plots shown in Fig. 3 proved that the thermal stability of the Gr-Ag/PNA nanocomposites had significantly increased. This suggests that the polymer backbones were significantly less susceptible to degradation in nanocomposites. According to the findings of FTIR and XRD

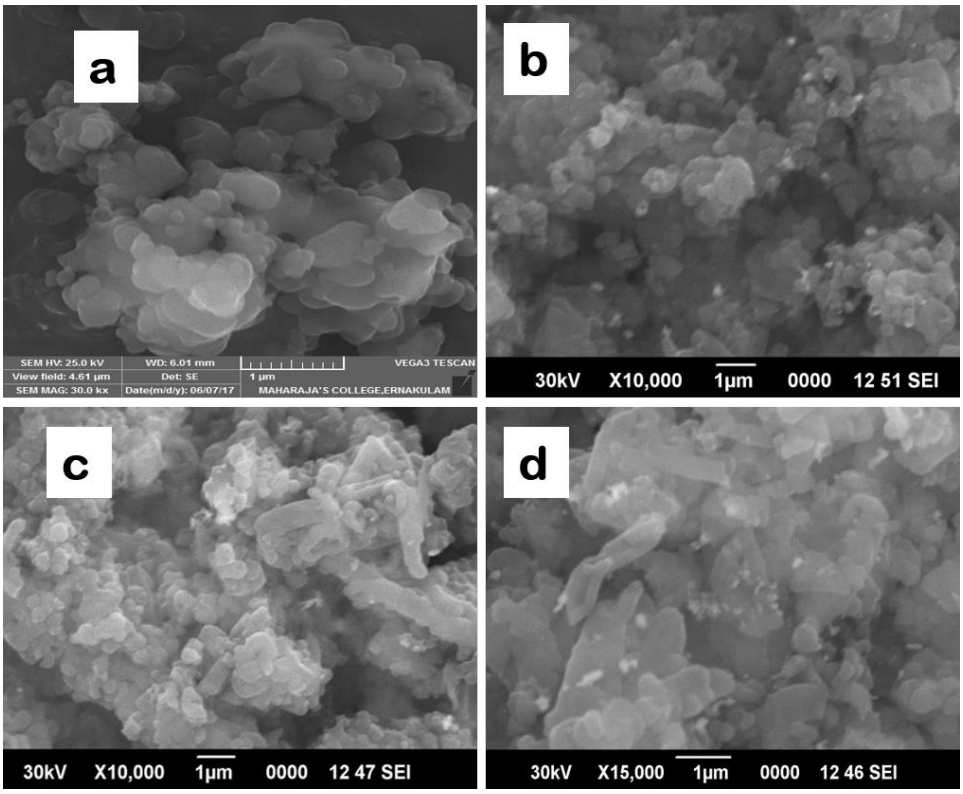

Fig. 4. SEM images of (a) PNA, (b) Gr-Ag-5/PNA, (c) Gr-Ag-10/PNA and (d) Gr-Ag-20/PNA

tests, this could have been caused by a structural reorganization of the polymer chains due to matrix interactions.

SEM and EDAX studies

Fig. 4 shows SEM images of PNA and Gr-Ag/PNA nanocomposites. PNA spheres appear as microspheres, whilst silver clusters appear as bright spots uniformly dispersed throughout their surfaces. Because of the interfacial interactions of AgNPs with PNA, the PNA microspheres seem to be more aggregated or clustered in the nanocomposite matrix. The EDAX analyses of the Gr-Ag-10/PNA verified the inclusion of silver in the PNA matrix via green synthesis (Supplemental Fig. S2). Because of contamination from the active oxidant APS, a minor quantity of S is also detected.

HRTEM analysis

Detailed morphological, topographical, and crystallographic information of the nanocomposites are obtained from HRTEM pictures and corresponding SAED patterns of PNA, AgNPs, and nanocomposites presented in Fig. 5. It was clear from the TEM studies that both in its pure form and in the nanocomposites obtained, PNA exhibited the similar sphere-like shape, and the AgNPs were uniformly dispersed throughout the surface of PNA spheres (Fig. 5a-f)). AgNPs were found to be just as crystallized when integrated, as indicated by their distinct SAED patterns with concentric rings (inset Fig. 5 a, c, e, and g).

EIS studies

PNA and Gr-Ag/PNA modified CPE were used in the EIS experiments to examine the influence of silver incorporation on the charge transfer properties of nanocomposites, and the findings are shown in Fig. 6 as Nyquist plots. All of the graphs looked the same, with a semicircle at low frequencies and a linear portion at higher frequencies. The diameter of each semicircle correlates to the resistance given to charge transfer across the corresponding electrode surfaces, and charge transfer resistance reduced as silver content increased, as demonstrated by the order of semicircle diameter Gr-Ag-20/PNA (R_{ct}= 2435 Ω) < Gr-Ag-10/PNA (R_{ct}= 3123 Ω) < Gr-Ag-5/PNA (R_{ct}= 3432 Ω) < PNA (R_{ct}= 4337 Ω). The Gr-Ag-20/PNA/CPE had the smallest diameter, implying that

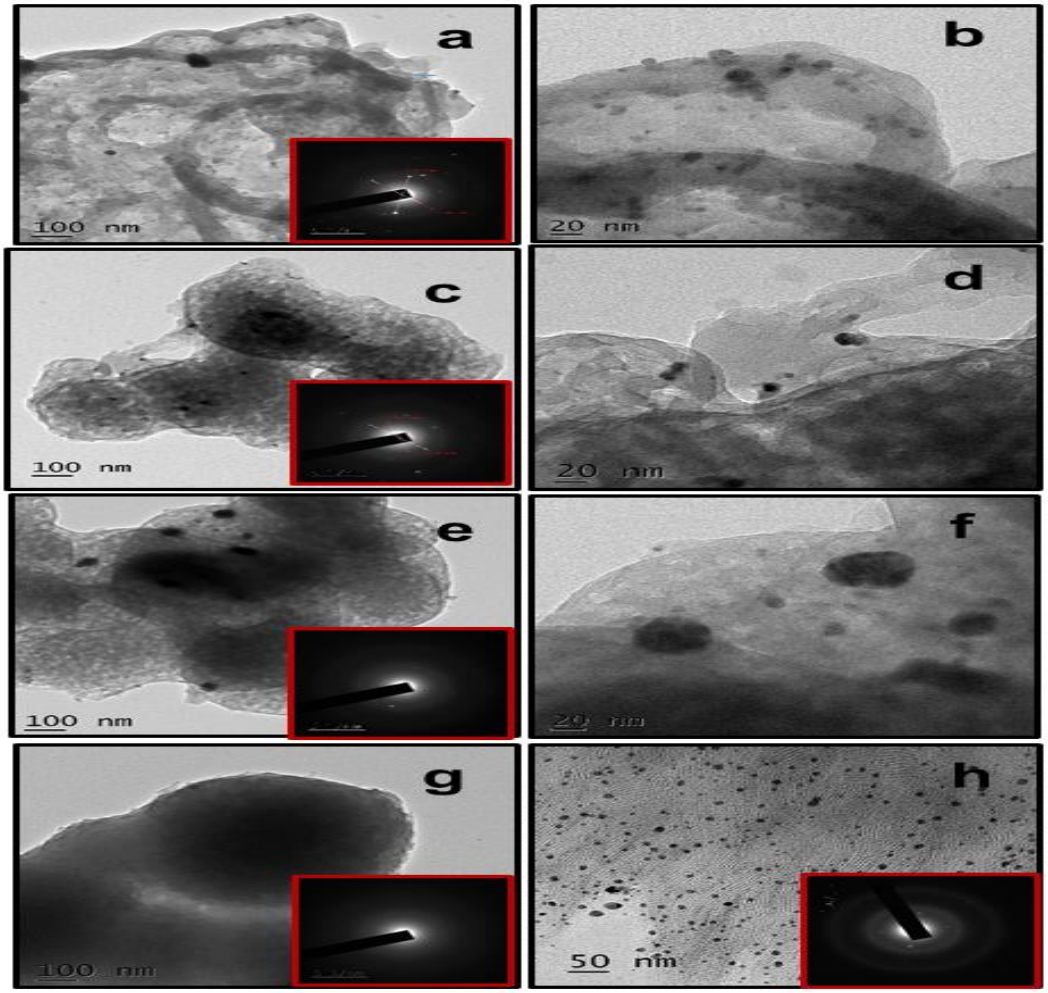

Fig. 5. TEM images of Gr-Ag-5/PNA (a and b) Gr-Ag-10/PNA (c and d) Gr-Ag-20/PNA (e and f), PNA (g) and AgNPs (h), and SAED patterns of Gr-Ag-5/PNA Gr-Ag-10/PNA, Gr-Ag-20/PNA, PNA, and AgNPs (inset a, c, e, f, g, and h, respectively)

it would have superior charge transfer kinetics, which might be due to the availability of a larger number of well-distributed catalytically active AgNPs over the large surface given by the PNA spheres.

Catalytic studies

The reduction of 4-NP with sodium borohydride as the reductant was studied catalytically in the presence of pristine PNA and Gr-Ag/PNA nanocomposites as heterogeneous catalysts. By keeping the reductant concentration much greater than that of 4-NP, the reactions were carried out under pseudo-first-order conditions. At regular time intervals, by separating the catalyst by centrifugation, the UV-Vis spectra of the reaction mixture were recorded, and the progress of the catalytic reaction was monitored (Supplemental Fig. S3). Since the reaction medium became alkaline with the addition of sodium borohydride, 4-nitrophenolate ions that have strong absorption at 400 nm were formed and the color of the solution became intensified. As the reaction progressed, 4-NP was reduced to colorless 4-aminophenol (4-AP), the color of the solution faded and the intensity of absorption at 400 nm lessened. For each catalyzed process, the absorbance values (A_t) at λmax (400 nm) were noted, and the plot $\ln(A_t/A_0)$ versus time was made. The pseudo-first-order rate constants (k_{app}) for each catalytic reaction were computed from the slope of the linear fit of each plot (Fig. 7(a-d)). Analyzing catalyzed reactions' kapp values allowed us to determine the influence of silver inclusion on the

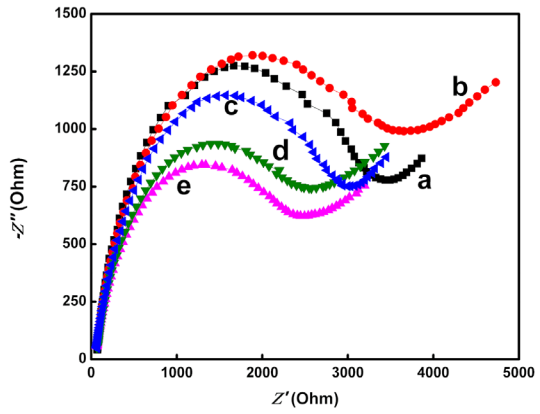

Fig.6 Nyquist plots of CPE (a), PNA/CPE (b), Gr-Ag-5/PNA/CPE (c), Gr-Ag-10/PNA/CPE (d), and Gr-Ag-20/PNA/CPE (e)

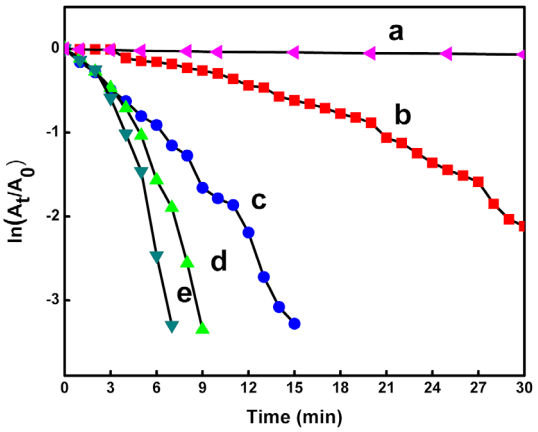

Fig.7. Plot of ln(At/Ao) of reduction of 4-NP catalyzed by PNA (a), Gr-Ag-5/PNA/CPE (b), Gr-Ag-10/PNA/CPE (c) and Gr-Ag-20/PNA/CPE (d)

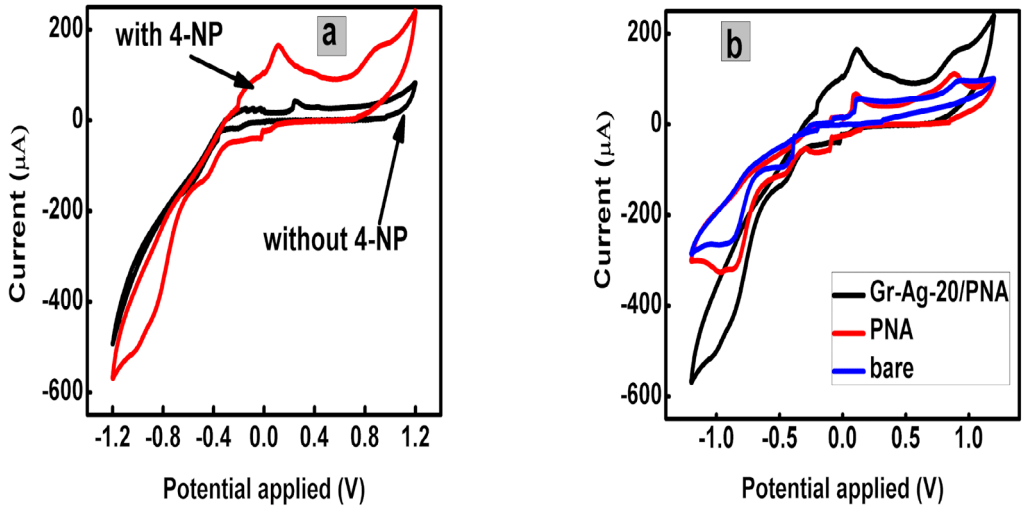

Fig.8. CV plots recorded without and with 4-NP (0.1 mM) in phosphate buffer in 50 mV/s over Gr-Ag-20/PNA/CPE (a) and CV plots recorded with 0.1 mM 4-NP at a scan rate of 50 mV/s over bare CPE, PNA/CPE and Gr-Ag-20/PNA/CPE (b)

Table 3.1. The k_{app} values calculated for the reduction of 4-NP under different catalytic conditions

Reaction condition (4-NP+$NaBH_4$)	Rate constant (K_{app}/min^{-1}) (RSD < 5%)
Without catalyst	0.00174
PNA	0.0647
Gr-Ag-5/PNA	0.1517
Gr-Ag-10/PNA	0.2513
Gr-Ag-20/PNA	0.4218

system's catalytic effectiveness. As a consequence of the integration of AgNPs over PNA, the catalytic activity is significantly enhanced, and the catalytic performance is directly proportional to the amount of silver integrated. Kapp was determined to be 0.0425 min^{-1} for pristine PNA, 0.1517 min^{-1} for Gr-Ag-5/PNA, 0.2513 min^{-1} for Gr-Ag-10/PNA and 0.4216 min^{-1} for Gr-Ag-20/PNA correspondingly (Table 3.1). A heterogeneous route has been proposed for the Gr-Ag/PNA or PNA-catalysed process, including the adhesion of reactants to the surface of the catalyst and electron transfer from the reductant to 4-NP. Over PNA-spheres, silver nanospheres are efficiently supported during

Table.1 Comparison of catalytic performance of Gr-Ag/PNA with some reported catalytic systems

Catalyst	[4-NP] 10^{-5} M	Rate constant (k_{app}) / min^{-1}	Reference
PNA-Ag (one step)	10	0.2981	[29]
Au/MMT/PANI	9	0.0792	[38]
Au-N *alata*	8	0.187	[45]
AgNPs-*N. alata*	8	0.195	[45]
Pt	20	0.0165	[46]
Pd	20	0.1088	[46]
polyacrylamide-Au	8	0.252	[47]
Ag-PANI	4	0.2046	[37]
Au-Fe_2O_3	-	0.882	[48]
Pd	10	0.1110	[49]
1.35% C_{60}-Au-TiO_2	20	0.083	[50]
Gr-Ag-5/PNA		0.1517	
Gr-Ag-10/PNA	10	0.2513	This work
Gr-Ag-20/PNA		0.4218	

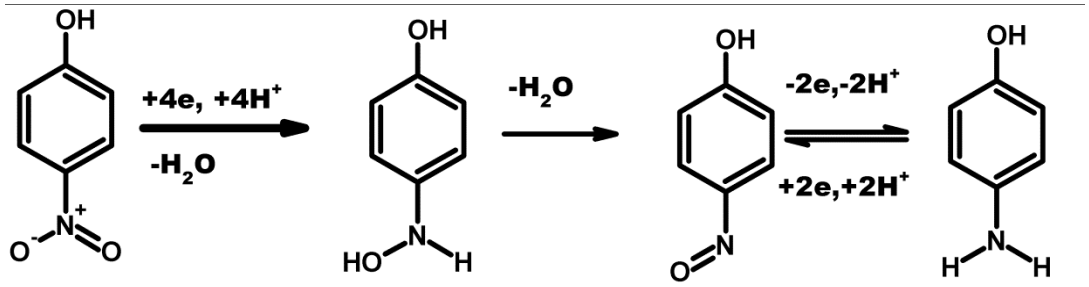

Fig.9. A plausible mechanism for electrochemical reduction of 4-NP over Gr-Ag/PNA/CPE

nanocomposite production, which might offer substantial surface areas for negatively charged nitrophenolate and borohydride ions to adhere to. Aside from that, the redox interaction between the catalytically active silver and PNA enhanced the electron transfer between the borohydride and nitrophenolate ions considerably quicker, reducing 4-NP to 4-AP much faster. A mechanistic approach for the conversion of 4-NP to 4-AP using Gr-Ag/PNA is suggested (Supplemental Fig. S4). As the quantity of silver loading rises, the more exposed active centers present over PNA accelerates electron transport between substrate and reductant, resulting in quicker 4-NP reduction. The Gr-Ag/PNA catalytic system's performance was compared to that of previous studies reported (Table 1), and it is evident that the demonstrated nanocomposites have high catalytic efficacy.

Electrocatalytic studies

To evaluate the electrochemical response and electrocatalytic performance of the Gr-Ag/PNA modified electrodes towards 4-NP reduction CV studies were performed with Gr-Ag-5/PNA, Gr-Ag-10/PNA, and Gr-Ag-20/PNA modified CPEs with and without 0.1 mM 4-NP solution and the corresponding CV plots are presented (Supplemental Fig. S5). The CV and EIS studies confirmed that among the Gr-Ag/PNA modifies CPEs, Gr-Ag-20/PNA have better charge transfer characteristics, improved electrochemical response, and excellent electrocatalytic capabilities Therefore, further investigations on electrocatalytic and electrochemical sensing were conducted with Gr-Ag-20/PNA/CPE. Comparison of CV profiles recorded at 50 mVs^{-1} with and without 0.1 mM

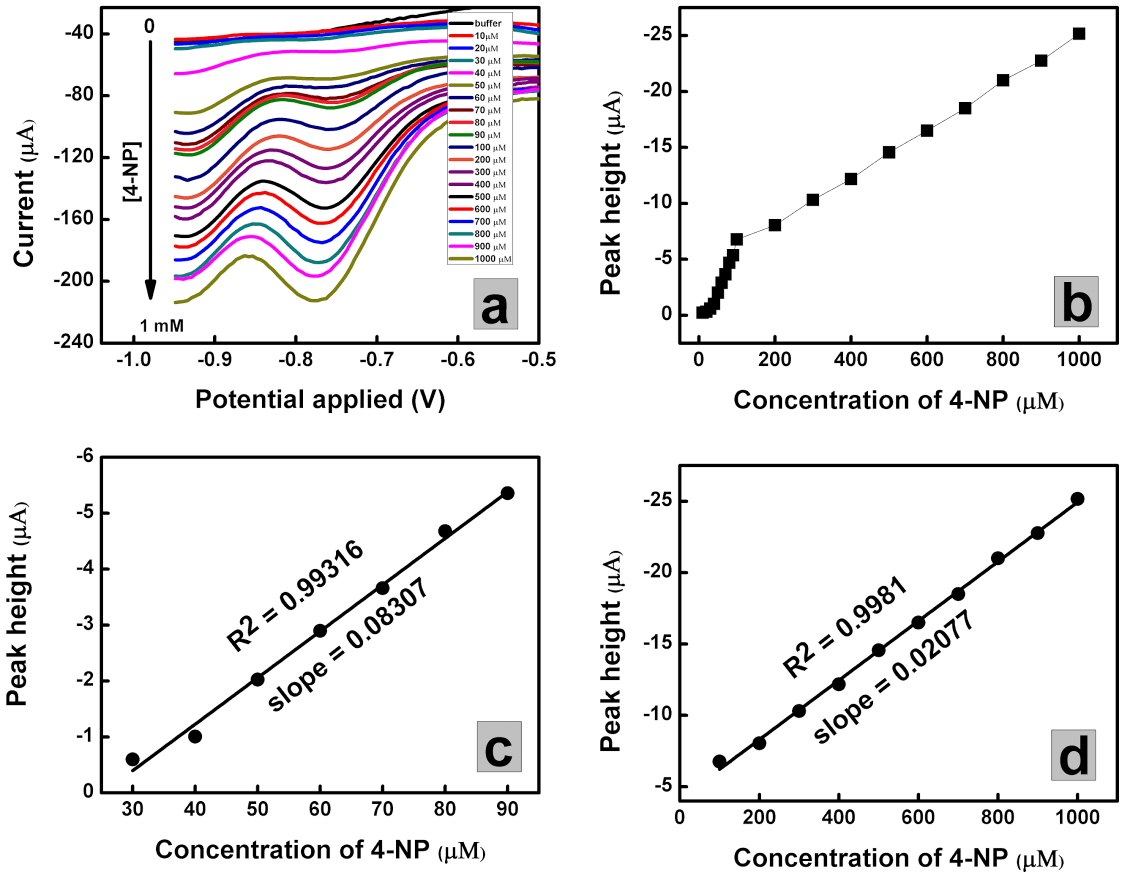

Fig.10. DPVs of (Gr-Ag-20/PNA/CPE)/CPE with increasing 4-NP concentrations (1- 1000 μM) in phosphate buffer solution against Ag/AgCl as reference electrode at potential

4-NP in buffer validated the electrocatalytic activity of Gr-Ag/PNA/CPE (Fig. 8a). As a result of the 4-NP reduction to hydroxyl aminophenol, Gr-Ag-20/PNA/CPE, PNA/CPE, and bare CPE displayed a significant reduction peak at -0.8 V. The hydroxylamine was oxidized to 4-nitrophenol, resulting in an anodic peak at +0.14V. There were no similar peaks at Gr-Ag-20/PNA when 4-NP was absent. CV profiles recorded with 4-NP were shown to have a three-fold increase in both anodic and cathodic peak currents compared to CV scans without 4-NP.

The electrocatalytic activity of bare CPE, PNA/CPE, and Gr-Ag-20/PNA/CPE was examined using CV measurements with 0.1 mM 4-NP in buffer at a scan rate of 50 mVs^{-1} (Fig. 8b). The Gr-Ag-20/PNA/CPE exhibited increased current response at specific redox peaks of 4-NP, as shown in Fig. 8b. The CV profiles revealed that the potential for reduction of 4-NP over Gr-Ag-20/PNA/CPE was at -0.80 V, whereas it was about 60 mV and 80 mV lower than that of PNA/CPE and bare CPE, respectively, and thus it was concluded that, even if the reduction occurs over all of these electrodes, the lower peak potential observed for Gr-Ag-20/PNA/CPE suggested its better electrocatalytic activity.

The effect of the applied scan rates on the CV response was utilized to study the nature of the electrocatalytic process over Gr-Ag-20/PNA. The CVs were recorded using 0.1 mM 4-NP at scan speeds ranging from 25 mVs-1 to 250 mVs-1, and the peak current values obtained during anodic and cathodic potential sweeps were plotted against the square root of the scan rates (Supplemental Fig. S5). The results revealed that the peak currents for reduction and oxidation increased linearly with scan rates, demonstrating that the overall electrochemical reaction of 4-NP at Gr-Ag-20/PNA was a diffusion-regulated process [51, 52].

According to the CV experiments, Gr-Ag-20/PNA on CPE had improved electrocatalytic response, which was ascribed to the unique

Table.2 Comparison of Gr-Ag-20/PNA/CPE based 4-NP with reported works

Electrode	Method	Linear range (μM)	LoD (μM)	Reference
Au-ZnS/GCE	DPV	0.15-2	0.320	[34]
AgNWs-PANI/GCE	DPV	0.6- 32	0.052	[17]
Nano-Au/GCE	CV	10-30	8	[53]
GNS-FePc/GCE.	DPV	100 - 700	10	[54]
RG-Fe_2O_3/GCE	SWV	0.2 - 10	0.86	[55]
PANi/GCE	DPV	6.7-112	3.2	[56]
MIP/GO	DPV	60-140	20	[57]
Ni-CoOx/GCE	DPV	7 - 682	4.8	[58]
ZnO/GCE	CV	10-1000	13	[59]
Gr-Ag-20/PNA/CPE	DPV	30-90	6.25	Present study
		100-1000		

electrostatic interaction of PNA and AgNPs with the electrode surface and 4-NP. As a result, it is recommended that Gr-Ag-20/PNA/CPE can be utilized for sensitive 4-NP determination at a comparatively low overpotential.

The electrochemical behavior estimated from the CV profile of 4-NP over the Gr-Ag-20/PNA/CPE was consistent with that reported by other authors. Fig. 9 depicts a probable mechanism for the electrochemical process of 4-NP over Gr-Ag/PNA/CPE based on prior findings and the results of several experiments used here.

Electrochemical sensing studies-DPV

DPV experiments were used to establish the sensitivity and detection limit (LoD) of a Gr-Ag-20/PNA/CPE-based 4-NP sensor. In the DPV plots of 4-NP in the concentration range of 1-1000 μM shown in Fig. 10 an obvious rise in peak current as the 4-NP concentration rises were found. The peak height (μA) was plotted against the corresponding 4-NP concentration (μM). In two continuous concentration regions, say 30 -100 μM and 100 -1000 μM, the calibration curve fits linearly with an acceptable correlation coefficient, and the corresponding linear regression equations are Ip =-0.0830 [4-NP] (μM) - 2.0959 (R^2 = 0.9931) and Ip = -0.0208 [4-NP] - 4.1526 (R^2 = 0.9981), respectively. From the calibration plot, the calculated LoD and sensitivity were 6.25 μM (Signal/Noise=3) and 423 μAmM^{-1} cm^{-2}, respectively.

The performance of the present sensor was compared with some reported electrochemical 4-NP sensors and presented in Table 2. The current 4-NP sensor has a large detection range, a low detection limit, and a high sensitivity, according to the research. The study is more appealing and noteworthy since it is simple to construct and uses less expensive electrode materials such as carbon paste and modifiers.

Reproducibility, stability, and selectivity

The DPV responses of Gr-Ag-20/PNA/CPE were recorded in 0.1 mM of 4-NP 10 times, and the relative standard deviation (RSD) of peak height was found to be within 3.4 %, suggesting high repeatability. The storage stability of Gr-Ag-20/PNA/CPE was also studied by detecting the current response of 0.1 mM 4-NP after a 10-day storage period, and it preserved 91 % of the original current, confirming that the Gr-Ag-20/PNA/CPE had significant storage stability. In the presence of interferents such as NaCl, KCl, KNO_3, $CaSO_4$, 4-AP, and 2-nitrophenol (2-NP), the selectivity of Gr-Ag-20/PNA/CPE towards 4-NP was evaluated, and the DPV current response was noted (Supplemental Fig. S6). The interference investigation indicated that inorganic salts had no effect on 4-NP detection, but other phenolic compounds produced a slight change in peak current. We have shown that Gr-Ag/

PNA can be easily synthesized via a cost-effective green route and that it performs well as a 4-NP sensor with a wide detection range, lower detection limit, and much better sensitivity. The work is more appealing compared to earlier reports because of its simplicity of manufacturing and usage of less expensive electrode materials and modifiers. This innovative and simple production of Ag/PNA nanocomposites is expected to open the way for the design and development of other useful PNA-based metal nanocomposites for a variety of applications.

CONCLUSION

In this study, AgNPs incorporated PNA nanocomposites were prepared using microwave-assisted photoreduction of silver ions in presence of dispersed PNA. Thus, we have shown a safer, more affordable, ecologically friendly, and scalable alternative to traditional physical, chemical, and microbiological approaches. We have also demonstrated the performance of prepared Ag/PNA nanocomposites was superior to or on par with that of similar composites produced using other processes. Dispersion of AgNP crystallites over the conjugated matrix of PNA could improve the charge transfer kinetics and sensing performances and the catalytic performance was substantially improved due to stabilization and synergistic interaction. between matrix components. We could easily modify the CPE surface with Gr-Ag/PNA without using any additional binder, and the GR-Ag/PNA modified electrodes demonstrated high sensitivity, higher selectivity, and a wide detection range towards voltammetric sensing of 4-NP. This work was noteworthy and appealing due to its high catalytic efficacy, good sensitivity, ease of fabrication, reusability, and cost-effectiveness. This facile manufacturing of Ag/PNA nanocomposites might lead to further PNA-based metal nanocomposites for a range of uses.

ACKNOWLEDGMENTS

The authors gratefully acknowledge the financial support provided to Femina K.S. by the University Grants Commission (under Faculty Development Program: Grant No. FIP/12th Plan/KLMG 009 TF 12 dated 20/04/2017), Government of India, and to Alex Joseph by the Kerala State Council for Science, Technology, and Environment (KSCSTE) Thiruvananthapuram, Kerala, India under the SARD scheme (Grant No.002/SARD/20). The authors would like to thank SAIF STIC in Cochin, Kerala, India, for the characterization facilities, as well as the Department of Chemistry at Newman College in Thodupuzha for the electrochemical investigations. The authors gratefully acknowledge Dr. Neena George of Maharajas College in Ernakulam, Kerala, India, for her critical suggestions during manuscript writing.

CONFLICT OF INTEREST

The author declares no conflict of interest

REFERENCE

1. Pareek V, Bhargava A, Gupta R, et al (2017) Synthesis and Applications of Noble Metal Nanoparticles: A Review. Adv Sci Eng Med 9:527-544. https://doi.org/10.1166/asem.2017.2027 https://doi.org/10.1166/asem.2017.2027
2. Syafiuddin A, Salmiati, Salim MR, et al (2017) A Review of Silver Nanoparticles: Research Trends, Global Consumption, Synthesis, Properties, and Future Challenges. J Chinese Chem Soc 64:732-756. https://doi.org/10.1002/jccs.201700067 https://doi.org/10.1002/jccs.201700067
3. Ghasemi Z, Abdi V, Sourinejad I (2020) Single-step biosynthesis of Ag/AgCl@TiO2 plasmonic nanocomposite with enhanced visible light photoactivity through aqueous leaf extract of a mangrove tree. Appl Nanosci 10:507-516. https://doi.org/10.1007/s13204-019-01149-4 https://doi.org/10.1007/s13204-019-01149-4
4. Basaleh AS, Mohamed RM (2020) Influence of doped silver nanoparticles on the photocatalytic performance of ZnMn2O4 in the production of methanol from CO2 photocatalytic reduction. Appl Nanosci 10:3865-3874. https://doi.org/10.1007/s13204-020-01468-x https://doi.org/10.1007/s13204-020-01468-x
5. Yadav S, Kumar N, Mari B, et al (2021) Ag/ZnO nano-structures synthesized by single-step solution combustion approach for the photodegradation of Cibacron Red and Triclopyr. Appl Nanosci 11:1977-1991. https://doi.org/10.1007/s13204-021-01943-z https://doi.org/10.1007/s13204-021-01943-z
6. Kumar THV, Sundramoorthy AK (2018) Non-Enzymatic Electrochemical Detection of Urea on Silver Nanoparticles Anchored Nitrogen-Doped Single-Walled Carbon Nanotube Modified Electrode. J Electrochem Soc 165:B3006-B3016. https://doi.org/10.1149/2.0021808jes https://doi.org/10.1149/2.0021808jes
7. Yang B, Liu Z, Guo Z, et al (2014) In situ green synthesis of silver-graphene oxide nanocomposites by using tryptophan as a reducing and stabilizing agent and their application in SERS. Appl Surf Sci 316:22-27. https://doi.org/10.1016/j.apsusc.2014.07.084 https://doi.org/10.1016/j.apsusc.2014.07.084
8. Singh A, Goswami A, Nain S (2020) Enhanced antibacterial activity and photo-remediation of toxic dyes using Ag/SWCNT/PPy based nanocomposite with core-shell structure. Appl Nanosci 10:2255-2268. https://doi.org/10.1007/s13204-020-01394-y https://doi.org/10.1007/s13204-020-01394-y
9. Atmeh M, Alcock-Earley BE (2011) A conducting polymer/Ag nanoparticle composite as a nitrate sensor. J Appl Electrochem 41:1341-1347. https://doi.org/10.1007/s10800-011-0354-4 https://doi.org/10.1007/s10800-011-0354-4
10. Spain E, Keyes TE, Forster RJ (2013) Polypyrrole-gold nanoparticle composites for highly sensitive

DNA detection. Electrochim Acta 109:102-109. https://doi.org/10.1016/j.electacta.2013.07.018 https://doi.org/10.1016/j.electacta.2013.07.018
11. Li S, Xiong J, Shen J, et al (2015) A novel hydrogen peroxide sensor based on Ag nanoparticles decorated polyaniline/graphene composites. J Appl Polym Sci 132:4-9. https://doi.org/10.1002/app.42409 https://doi.org/10.1002/app.42409
12. Stejskal J (2013) Conducting polymer-silver composites. Chem Pap 67:814-848. https://doi.org/10.1017/S0025315400040285 https://doi.org/10.1017/S0025315400040285
13. Boeva ZA, Sergeyev VG (2014) Polyaniline: Synthesis, properties, and application. Polym Sci Ser C 56:144-153. https://doi.org/10.1134/s1811238214010032 https://doi.org/10.1134/S1811238214010032
14. Ćirić-Marjanović G (2013) Recent advances in polyaniline research: Polymerization mechanisms, structural aspects, properties and applications. Synth Met 177:1-47. https://doi.org/https://doi.org/10.1016/j.synthmet.2013.06.004 https://doi.org/10.1016/j.synthmet.2013.06.004
15. Saini D, Basu T (2012) Synthesis and characterization of nanocomposites based on polyaniline-gold/graphene nanosheets. Appl Nanosci 2:467-479. https://doi.org/10.1007/s13204-012-0059-y https://doi.org/10.1007/s13204-012-0059-y
16. Pillalamarri SK, Blum FD, Tokuhiro AT, Bertino MF (2005) One-pot synthesis of polyaniline - Metal nanocomposites. Chem Mater 17:5941-5944. https://doi.org/10.1021/cm050827y https://doi.org/10.1021/cm050827y
17. Zhang C, Govindaraju S, Giribabu K, et al (2017) AgNWs-PANI nanocomposite based electrochemical sensor for detection of 4-nitrophenol. Sensors Actuators, B Chem 252:616-623. https://doi.org/10.1016/j.snb.2017.06.039 https://doi.org/10.1016/j.snb.2017.06.039
18. Ali F, Khan SB, Kamal T, et al (2017) Chitosan coated cotton cloth supported zero-valent nanoparticles: Simple but economically viable, efficient and easily retrievable catalysts. Sci Rep 7:1-16. https://doi.org/10.1038/s41598-017-16815-2 https://doi.org/10.1038/s41598-017-16815-2
19. Jyoti K, Singh A (2016) Green synthesis of nanostructured silver particles and their catalytic application in dye degradation. J Genet Eng Biotechnol 14:311-317. https://doi.org/10.1016/j.jgeb.2016.09.005 https://doi.org/10.1016/j.jgeb.2016.09.005
20. Saikia P, Miah AT, Das PP (2017) Highly efficient catalytic reductive degradation of various organic dyes by Au/CeO2-TiO2 nano-hybrid. J Chem Sci 129:81-93. https://doi.org/10.1007/s12039-016-1203-0 https://doi.org/10.1007/s12039-016-1203-0
21. Shah MR, Sherazi STH, Kalwar NH, et al (2015) Catalytic Reductive Degradation of Methyl Orange Using Air Resilient Copper Nanostructures. J Nanomater 2015:1-12. https://doi.org/10.1155/2015/136164 https://doi.org/10.1155/2015/136164
22. Yu C, Tang J, Liu X, et al (2019) Green biosynthesis of silver nanoparticles using eriobotrya japonica (thunb.) leaf extract for reductive catalysis. Materials (Basel) 12:. https://doi.org/10.3390/ma12010189 https://doi.org/10.3390/ma12010189
23. Li, Xiang, Ta, Na; Sun C (2005) Electrochemical polymerization of 1-naphthylamine and properties of poly-1-naphthylamine. Bull Electrochem 21:173-177
24. Tran MT, Nguyen THT, Vu QT, Nguyen MV (2016) Properties of poly(1-naphthylamine)/Fe3O4 composites and arsenic adsorption capacity in wastewater. Front Mater Sci 10:56-65. https://doi.org/10.1007/s11706-016-0320-5 https://doi.org/10.1007/s11706-016-0320-5
25. Pei LZ, Ma Y, Qiu FL, et al (2018) In-situ synthesis of polynaphthylamine/graphene composites for the electrochemical sensing of benzoic acid. Mater Res Express 6:15053. https://doi.org/10.1088/2053-1591/aae96e https://doi.org/10.1088/2053-1591/aae96e
26. Shaffie KA (2000) Preparation and characterization of polynaphthylamine (PNA) as a novel conducting polymer. J Appl Polym Sci 77:988-992 https://doi.org/10.1002/1097-4628(20000801)77:5<988::AID-APP5>3.0.CO;2-V
27. Saidu FK, Joseph A, Varghese EV, Thomas GV (2019) Silver nanoparticles-embedded poly(1-naphthylamine) nanospheres for low-cost non-enzymatic electrochemical H2O2 sensor. Polym Bull 77:5825-5846. https://doi.org/10.1007/s00289-019-03053-x https://doi.org/10.1007/s00289-019-03053-x
28. Saidu FK, Joseph A, Varghese EV, Thomas GV (2019) Characterization and electrochemical studies on poly(1-naphthylamine)-graphene oxide nanocomposites prepared by in situ chemical oxidative polymerization. J Solid State Electrochem 23:2897-2906. https://doi.org/10.1007/s10008-019-04380-9 https://doi.org/10.1007/s10008-019-04380-9
29. Saidu FK, Joseph A, Thomas G V (2019) Synthesis of novel poly(1- naphthylamine)- silver nanocomposites and its catalytic studies on reduction of 4-nitrophenol and methylene blue. J Appl Polym Sci 137:48318-48328. https://doi.org/10.1002/app.48318 https://doi.org/10.1002/app.48318
30. Jadoun S, Verma A, Ashraf SM, Riaz U (2017) A short review on the synthesis, characterization, and application studies of poly(1-naphthylamine): a seldom explored polyaniline derivative. Colloid Polym Sci 295:1443-1453. https://doi.org/10.1007/s00396-017-4129-2 https://doi.org/10.1007/s00396-017-4129-2
31. Roy BC, Gupta MD, Bhowmik L, Ray JK (2003) Synthesis and characterization of conducting poly (1-aminonaphthalene), poly (2-aminonaphthalene) and poly (aniline-co-1-aminonaphthalene). Bull Mater Sci 26:633-637. https://doi.org/10.1007/BF02704328 https://doi.org/10.1007/BF02704328
32. Kovacic P, Somanathan R (2014) Nitroaromatic compounds: Environmental toxicity, carcinogenicity, mutagenicity, therapy and mechanism. J Appl Toxicol 34:810-824. https://doi.org/10.1002/jat.2980 https://doi.org/10.1002/jat.2980
33. Francis S, Joseph S, Koshy EP, Mathew B (2017) Green synthesis and characterization of gold and silver nanoparticles using Mussaenda glabrata leaf extract and their environmental applications to dye degradation. Environ Sci Pollut Res 24:17347-17357. https://doi.org/10.1007/s11356-017-9329-2 https://doi.org/10.1007/s11356-017-9329-2
34. Kim HJ, Lee JB, Giribabu K, et al (2018) Electrochemical Sensors Based on Au-ZnS Hybrid Nanorods with Au-Mediated Efficient Electron Relay. ACS Sustain Chem Eng 7:4094-4102. https://doi.org/10.1021/acssuschemeng.8b05603 https://doi.org/10.1021/acssuschemeng.8b05603
35. Qiu C, Du J, Huang L, et al (2009) Electrochemical sensor for detection of p-nitrophenol based on nanoporous gold. Electrochem commun 11:1365-1368. https://doi.org/10.1016/j.elecom.2009.05.004

https://doi.org/10.1016/j.elecom.2009.05.004
36. Song C, Yu K, Yin H, et al (2014) Highly efficient field emission properties of a novel layered VS2/ZnO nanocomposite and flexible VS2nanosheet. J Mater Chem C 2:4196-4202. https://doi.org/10.1039/c4tc00025k https://doi.org/10.1039/C4TC00025K
37. Yuan C, Xu Y, Zhong L, et al (2013) Heterogeneous silver-polyaniline nanocomposites with tunable morphology and controllable catalytic properties. Nanotechnology 24:185602-185611. https://doi.org/10.1088/0957-4484/24/18/185602 https://doi.org/10.1088/0957-4484/24/18/185602
38. Xia Y, Li T, Ma C, et al (2014) Au/montmorillonite/polyaniline nanoflakes: Facile fabrication by self-assembly and application as catalyst. RSC Adv 4:20516-20520. https://doi.org/10.1039/c4ra02225d https://doi.org/10.1039/C4RA02225D
39. Ma B, Wang M, Tian D, et al (2015) Micro/nano-structured polyaniline/silver catalyzed borohydride reduction of 4-nitrophenol. RSC Adv 5:41639-41645. https://doi.org/10.1039/C5RA05396J https://doi.org/10.1039/C5RA05396J
40. Sepasgozar SME, Mohseni S, Feizyzadeh B, Morsali A (2021) Green synthesis of zinc oxide and copper oxide nanoparticles using Achillea Nobilis extract and evaluating their antioxidant and antibacterial properties. Bull Mater Sci 44:129. https://doi.org/10.1007/s12034-021-02419-0 https://doi.org/10.1007/s12034-021-02419-0
41. Bozetine H, Meziane S, Aziri S, et al (2021) Facile and green synthesis of a ZnO/CQDs/AgNPs ternary heterostructure photocatalyst: study of the methylene blue dye photodegradation. Bull Mater Sci 44:64. https://doi.org/10.1007/s12034-021-02353-1 https://doi.org/10.1007/s12034-021-02353-1
42. Asariha M, Chahardoli A, Karimi N, et al (2020) Green synthesis and structural characterization of gold nanoparticles from Achillea wilhelmsii leaf infusion and in vitro evaluation. Bull Mater Sci 43:57. https://doi.org/10.1007/s12034-019-2005-z https://doi.org/10.1007/s12034-019-2005-z
43. Saidu FK, Mathew A, Parveen A, et al (2019) Novel green synthesis of silver nanoparticles using clammy cherry (Cordia obliqua Willd) fruit extract and investigation on its catalytic and antimicrobial properties. SN Appl Sci 1:1368-1380. https://doi.org/10.1007/s42452-019-1302-x https://doi.org/10.1007/s42452-019-1302-x
44. Gupta R, Das Gupta G (2018) Isolation and characterization of flavonoid glycoside from Cordia obliqua Willd. leaf. Int J Green Pharm 17:73-79
45. Francis S, Joseph S, Koshy EP, Mathew B (2017) Synthesis and characterization of multifunctional gold and silver nanoparticles using leaf extract of: Naregamia alata and their applications in the catalysis and control of mastitis. New J Chem 41:14288-14298. https://doi.org/10.1039/c7nj02453c https://doi.org/10.1039/C7NJ02453C
46. Islam MT, Saenz-Arana R, Wang H, et al (2018) Green synthesis of gold, silver, platinum, and palladium nanoparticles reduced and stabilized by sodium rhodizonate and their catalytic reduction of 4-nitrophenol and methyl orange. New J Chem 42:6472-6478. https://doi.org/10.1039/c8nj01223g https://doi.org/10.1039/C8NJ01223G
47. Salaheldin HI (2017) Comparative catalytic reduction of 4-nitrophenol by polyacrylamide-gold nanocomposite synthesized by hydrothermal autoclaving and conventional heating routes. Adv Nat Sci Nanosci Nanotechnol 8:45001 https://doi.org/10.1088/2043-6254/aa8542 https://doi.org/10.1088/2043-6254/aa8542
48. Chang YC, Chen DH (2009) Catalytic reduction of 4-nitrophenol by magnetically recoverable Au nanocatalyst. J Hazard Mater 165:664-669. https://doi.org/10.1016/j.jhazmat.2008.10.034 https://doi.org/10.1016/j.jhazmat.2008.10.034
49. Kora AJ, Rastogi L (2018) Green synthesis of palladium nanoparticles using gum ghatti (Anogeissus latifolia) and its application as an antioxidant and catalyst. Arab J Chem 11:1097-1106. https://doi.org/10.1016/j.arabjc.2015.06.024 https://doi.org/10.1016/j.arabjc.2015.06.024
50. Islam MT, Jing H, Yang T, et al (2018) Fullerene stabilized gold nanoparticles supported on titanium dioxide for enhanced photocatalytic degradation of methyl orange and catalytic reduction of 4-nitrophenol. J Environ Chem Eng 6:3827-3836. https://doi.org/10.1016/j.jece.2018.05.032 https://doi.org/10.1016/j.jece.2018.05.032
51. Chang G, Luo Y, Lu W, et al (2012) Ag nanoparticles decorated polyaniline nanofibers: Synthesis, characterization, and applications toward catalytic reduction of 4-nitrophenol and electrochemical detection of H 2O 2 and glucose. Catal Sci Technol 2:800-806. https://doi.org/10.1039/c2cy00454b https://doi.org/10.1039/c2cy00454b
52. Yang G (2015) One-pot preparation of reduced graphene oxide/silver nanocomposite and its application in the electrochemical determination of 4-nitrophenol. Int J Electrochem Sci 10:9632-9640
53. Olorundare FOG, Nkosi D, Arotiba OA (2016) Voltammetric determination of nitrophenols at a nickel dimethylglyoxime complex - gold nanoparticle modified glassy carbon electrode. Int J Electrochem Sci 11:7318-7332. https://doi.org/10.20964/2016.09.47 https://doi.org/10.20964/2016.09.47
54. Devasenathipathy R, Mani V, Chen SM, et al (2015) Determination of 4-nitrophenol at iron phthalocyanine decorated graphene nanosheets film modified electrode. Int J Electrochem Sci 10:1384-1392
55. Cheng Y, Li Y, Li D, et al (2017) A sensor for detection of 4-nitrophenol based on a glassy carbon electrode modified with a reduced graphene oxide/Fe304 nanoparticle composite. Int J Electrochem Sci 12:7754-7764. https://doi.org/10.20964/2017.08.08 https://doi.org/10.20964/2017.08.08
56. Suresh R, Giribabu K, Manigandan R, et al (2016) Polyaniline Nanorods: Synthesis, Characterization, and Application for the Determination of para-Nitrophenol. Anal Lett 49:269-281. https://doi.org/10.1080/00032719.2015.1067815 https://doi.org/10.1080/00032719.2015.1067815
57. Saadati F, Ghahramani F, Shayani-jam H, et al (2018) Synthesis and characterization of nanostructure molecularly imprinted polyaniline/graphene oxide composite as highly selective electrochemical sensor for detection of p-nitrophenol. J Taiwan Inst Chem Eng 86:213-221. https://doi.org/10.1016/j.jtice.2018.02.019 https://doi.org/10.1016/j.jtice.2018.02.019
58. Asadpour-Zeynali K, Delnavaz E (2017) Electrochemical synthesis of nickel-cobalt oxide nanoparticles on the glassy carbon electrode and its application for the voltammetric determination of 4-nitrophenol. J Iran Chem Soc 14:2229-2238. https://doi.org/10.1007/s13738-017-1159-0 https://doi.org/10.1007/s13738-017-1159-0
59. Sinhamahapatra A, Bhattacharjya D, Yu JS (2015) Green fabrication of 3-dimensional flower-shaped zinc glycerolate and ZnO microstructures for p-nitrophenol sensing. RSC Adv 5:37721-37728. https://doi.org/10.1039/c5ra06286a https://doi.org/10.1039/C5RA06286A